Oceanologia, 66 (4)/2024, 66405

https://doi.org/10.5697/VIVV8745

A study of upper ocean characteristics in response to the three intense re-curving tropical cyclones from the Arabian Sea using satellite and in situ measurements

Adarsh Dube[1,4,*], Ajeet Ku Maurya[2], Rajesh Singh[3], T. Dharmaraj[1]

Abstract

We present the sea surface temperature (SST), latent heat flux (LHF), and sensible heat flux (SHF) studies of three tropical cyclones in the Indian subcontinent region. These three tropical cyclones were scrutinized based on their intensity scale ranging from Category 2 (Very Severe Cyclonic Storm, VSCS) to Category 5 (Super Cyclonic Storm, SuCS) on a hurricane scale (IMD scale). VSCS Vayu, SuCS Kyarr, and ESCS (Extremely Severe Cyclonic Storm) Maha formed over the Arabian Sea in June, October, and November 2019, respectively. There is a 2°C to 4°C difference in the SST during the pre- and post-cyclone period along the best track. The maximum reductions in SST up to 8°C have occurred in the region from where the cyclones have re-curved. The enthalpy fluxes (LHF and SHF) are highest at 280 W/m^2 around the cyclone's best track and follow the same direction of the cyclone development. Prior flux changes in the cyclone region may have a role in directing the cyclone's best track. Argo floats within 1° from the best track revealed that pre-cyclone SST was warmer at the surface than post-cyclone SST. The sub-surface SST at a depth of 100–150 m suggests a warming of the ocean in the post-cyclone period near and adjacent to cyclone intensification regions due to the upwelling of the warm subsurface waters. The upper ocean response is crucial to studying the increasing intensity of TCs and the re-curvature of its best track over the Arabian Sea.

Keywords

Tropical cyclones re-curvature; Argo floats; SST; Enthalpy fluxes

[1] *Indian Institute of Tropical Meteorology, Pune, India*
[2] *Department of Physics, Babasaheb Bhimrao Ambedkar University, Lucknow, India*
[3] *K.S. Krishnan Geomagnetic Research Laboratory, IIG, Prayagraj, India*
[4] *India Meteorological Department, Pune, India*
***Correspondence**: adarsh.dube92@gmail.com (A. Dube)

Received: 14 April 2024; **revised**: 3 September 2024; **accepted**: 6 September 2024

1. Introduction

Tropical Cyclones (TCs) are synoptic scale weather disturbances that wreak havoc in the coastal regions of the world with accompanying winds, intense precipitation, storm surge, etc., (Zhao et al, 2018; Cao et al, 2021; Cai et al., 2022). The frequency of TCs over the Arabian Sea (AS) has recently increased during pre- and post-monsoon periods (Evan et al., 2011; Murakami et al, 2017; Hari et al., 2021). By utilizing climate model experiments and observation data Hari et al. (2021) have shown that anthropogenic warming in the last decade may further enhance the frequency of TCs over AS. Also, the lessening of the vertical wind shear caused by the warming of the South Atlantic Ocean helps in cyclone genesis over AS (Hari et al., 2021). Further, the intensification of the TCs depends upon many processes related to microphysical effect and boundary layer phenomena that include several parameters such as angular momentum and sea surface temperature (Krishnamurthy et al., 2005; Bhaskar Rao et al., 2009).

Sea surface temperature (SST) plays a key role in the evolution of tropical cyclones from their genesis to intensification and dissipation (Kotal et al., 2009). SST is used as a gauge for measuring the tropical and extratropical cyclone intensity. The number of such cyclones (increasing in frequency and intensity) differ over regional scales, where favorable conditions include rising SST supported by mid-troposphere dryness and wind shear (IPCC, 2014; Chand et al., 2022). Global warming can easily enhance the TC intensity, as SST modulates the TC's energy and helps its intensification (Sun et al., 2017; Wahiduzzaman et al., 2022). Adding to SST's impact on tropical cyclone intensity, it also modulates the cyclone's best track (Katsube and Inatsu, 2016). They have found that the activities of

TCs are accelerated over regions with warmer SST. A study of TC over the Bay of Bengal has demonstrated that ocean basins with warmer sea surface conditions help deviate the cyclone's best track northward (Mohanty et al. 2019). In a modeling approach, performed with SST derived from the satellite and Reynold's weekly averaged SST, it is found that the SST derived from the satellite has improved the TC intensity prediction due to enhanced prediction of latent heat flux (LHF) and sensible heat flux (SHF) (Bongirwar et al., 2011).

Enthalpy fluxes enhance the formation and intensification of tropical cyclones over the ocean (Emanuel 1986; Craig and Gray 1996). A few case studies have found that LHF combined with SHF rapidly intensifies the TCs (Gautam et al. 2005; Lin et al. 2009; Jaimes et al. 2015). Many previous works have revealed that a decrease in SST of up to 1°C in the inner core of a cyclone would efficiently increase the total enthalpy flux by 40% or more (Cione and Uhlhorn, 2003). A study of the upper ocean response to TCs reported that amongst the two enthalpy fluxes, SHF has a prominent role in forcing the storm through its intense stage (Ma et al., 2015, 2018). Re-stratification of horizontal layers preceding a TC is caused by turbulent fluxes (LHF and SHF) at the ocean-air interface creating thermal and salinity fronts that sustain cyclone intensification (Navaneeth et al., 2019). A study based on numerical modeling in the Bay of Bengal urges more studies dealing with analyses based on in situ observations to understand the characteristics of the upper ocean during the cyclone (Neetu et al., 2012).

The dynamics of the structure of the upper ocean upon the overpasses of cyclones can be decoded well by increasing the number of in situ observations clubbed together with the synoptic remote-sensing observations (Navaneeth et al., 2019). Utilizing the observations based on in situ platforms such as moored buoys and Argo together with satellite-based observations, the contrasting response of variability in the upper ocean structure of the Bay of Bengal to the cyclone Nargis (Category 4) and Laila (Category 1) was recorded (Maneesha et al., 2012). A study on tropical cyclones from the Bay of Bengal reported a possibility to quantify the role of salinity and temperature in cyclone-induced restraint in upper ocean cooling but asked for a greater number of measurements of temperature and salinity profiles from in situ observations in the upper ocean with reasonable temporal and spatial coverage (Neetu et al., 2012). The unfolding of temperature and depth of the mixed layer estimated from Argo data supports the findings that tropical cyclone-induced effects are seen for a longer duration in the sub-surface layers while the surface layer returns to pre-cyclone condition rather quickly (Park et al., 2011).

TCs in the North Indian Ocean (NIO) hit a record high of six in number in the year 2019. The Arabian Sea witnessed a never-seen occurrence of four severe cyclones in 2019 against the climatological record of one per year from 1891–2018 (IMD). The previous studies in the NIO have focused on the response of the upper ocean to the TCs but these studies are limited to the region of Bay of Bengal. In this study, we approach the gap of studies of TCs from the Arabian Sea. Adding to it, the phenomenon of re-curvature of cyclone tracks over the Arabian Sea is new. Re-curving cyclones are less studied except for a few (Shyamala et al., 2001, Aiyyer, 2015). Re-curving tropical cyclones are very difficult to forecast since their physics and dynamics are much less studied in localized space and time (Aiyyer, 2015). The dependencies of the cyclone track on the SST and flux in the region are analyzed for studying the changing AS dynamics' role in increasing instances of TC formation and TC track re-curvature.

2. Data

TC's best track data were obtained from the Indian Meteorological Department (http://mausam.imd.gov.in). This dataset comprises details of tropical cyclones in the North Indian Ocean (geo-latitude 0–30N, geo-longitude 50E–100E) from the year 1982 onwards. This dataset has time, position (latitude and longitude of the storm center), sea level pressure, maximum sustained wind speed at the surface during all stages of the TC, and number of points in the TC tracks. The dataset is archived for each cyclone at 3-hour intervals for their entire period of evolution from genesis to decay after landfall. It also gives a measure of TC intensity by assigning globally acknowledged T-numbers.

The SST data was obtained from the Group for High-Resolution Sea Surface Temperature (GHRSST). This dataset is hosted at the GHRSST data archiving center at NASA JPL and can be retrieved from the website https://podaac.jpl.nasa.gov/dataset/MURJPL-L4-GLOB-v4.1. In this study, L4 gap-free gridded products are used. This dataset has an advantage over others in that it has a resolution of 0.018 degrees and uses microwave sensors which help remove cloud components from measuring SST. The dataset is available in a globally gridded format and is archived in daily files. We have utilized the SST data for 2019 and for June, October, and November in this study.

Enthalpy flux measurements (LFH and SFH) were retrieved from the dataset available at Ocean Heat Fluxes Climate Data Record (CDR) maintained by NOAA. It can be accessed from the year 1988. It is archived every 3 hours and it has a 0.02 degree spatial resolution. It is estimated that all the regions of global oceans are ice-free. The dataset can be retrieved from the website https://www.ncdc.noaa.gov/cdr/atmospheric/oceanheat-fluxes. However, the dataset is associated with a shortcoming in that it puts an upper limit on the wind speed at 45 m s^{-1} due to unknown values outside of the experimental data range of the neural network used to calculate the heat fluxes. However, we have used this dataset in the present work to evaluate the close dependency of these fluxes on the tropical cyclone intensity.

The Argo profiles adjacent to the cyclone's best track were utilized for in situ observations. Their dataset was obtained from the operational oceanography archive at http://www.coriolis.eu.org. Argo floats are deployed in the open ocean to measure the temperature and salinity of the ocean vertical profile up to a depth of 2 km. The dataset used in this study comprises a global array of at least 3000 such free-drifting profiling floats. The observation and monitoring of the physical parameters of the upper ocean is possible through this network. Their data is relayed to the collection center and is available for public use in a short time upon reception.

3. Description of tropical cyclones

Figure 1 shows the tropical cyclone best track latitudes and longitudes color-coded on the map, Vayu (red), Kyarr (black), and Maha (blue) respectively. VSCS Vayu evolved from an already existing low over geo latitude 11.7N and longitude 71E at 0300 UTC hours of 9 June 2019. The estimated Tropical Cyclone Heat Potential (TCHP) over the region was observed to be 100–110 KJ/cm^2 (IMD Report). It moved further northwest and grew into a deep depression (DD) at ~0600 UTC and evolved into a cyclonic storm (CS) Vayu at 1800 UTC hours of 10 June 2019 over east central of AS. It then moved northwards and intensified into a severe cyclonic storm (SCS) at 1200 UTC hours on 11 June and into a very severe cyclonic storm (VSCS) at 1800 UTC hours over the east-central AS. The maximum wind speed of the cyclone was 165 kmph moving through 13 June for 24-hour periods over geo latitude 20–21N and longitude 69–70E. Figure 2a shows the sea level pressure at the center and sustained wind speed variations during VSCS Vayu. It gradually started re-curving towards the northeast from 1200 UTC hours of 16 June. On 17 June 2019, VSCS Vayu dissipated over the western coasts of India around geo latitude 22.5N and longitude 67.8E.

SuCS Kyarr intensified from a depression over geo latitude 20.4N and longitude 70.4E on 17 October 2019. It was the 1st SuCS that occurred over the Arabian Sea during the post-monsoon season from 1965 to 2019 (IMD Report). Its growth into a Cyclonic Storm (CS) Kyarr transpired at 0000 UTC hours of 25 October over latitude 15.9N and longitude 71.5E. It evolved into a Severe Cyclonic Storm (SCS) at 1200 UTC hours on 25 October moving 0.4 degrees N and 0.2 degrees E from the CS. Thereafter, it re-curved to the west of northwest and grew into a very severe cyclonic storm (VSCS) over geo latitude 16.5N and longitude 70.8E at 0000 UTC hours of 26 October. It continued to move in the same direction and evolved further into an Extremely Severe Cyclonic Storm (ESCS) at 1500 UTC hours on 26

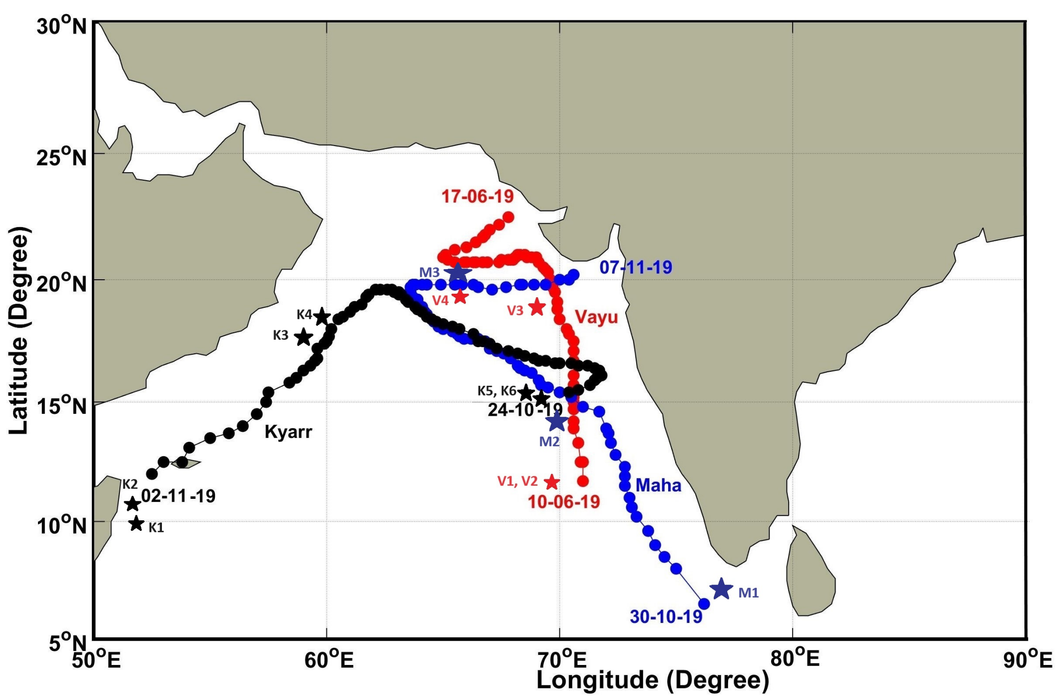

Figure 1. The best track of the tropical cyclones formed over the Arabian Sea in 2019. The observed storm track is shown as the Super Cyclone (SC) Kyarr (in black) (Category 4), Extremely Severe Cyclone Storm (ESCS) Maha (in blue) (Category 3), and Very Severe Cyclonic Storm (VSCS) Vayu (in Red). The location of scrutinized Argo floats is marked along the cyclone tracks.

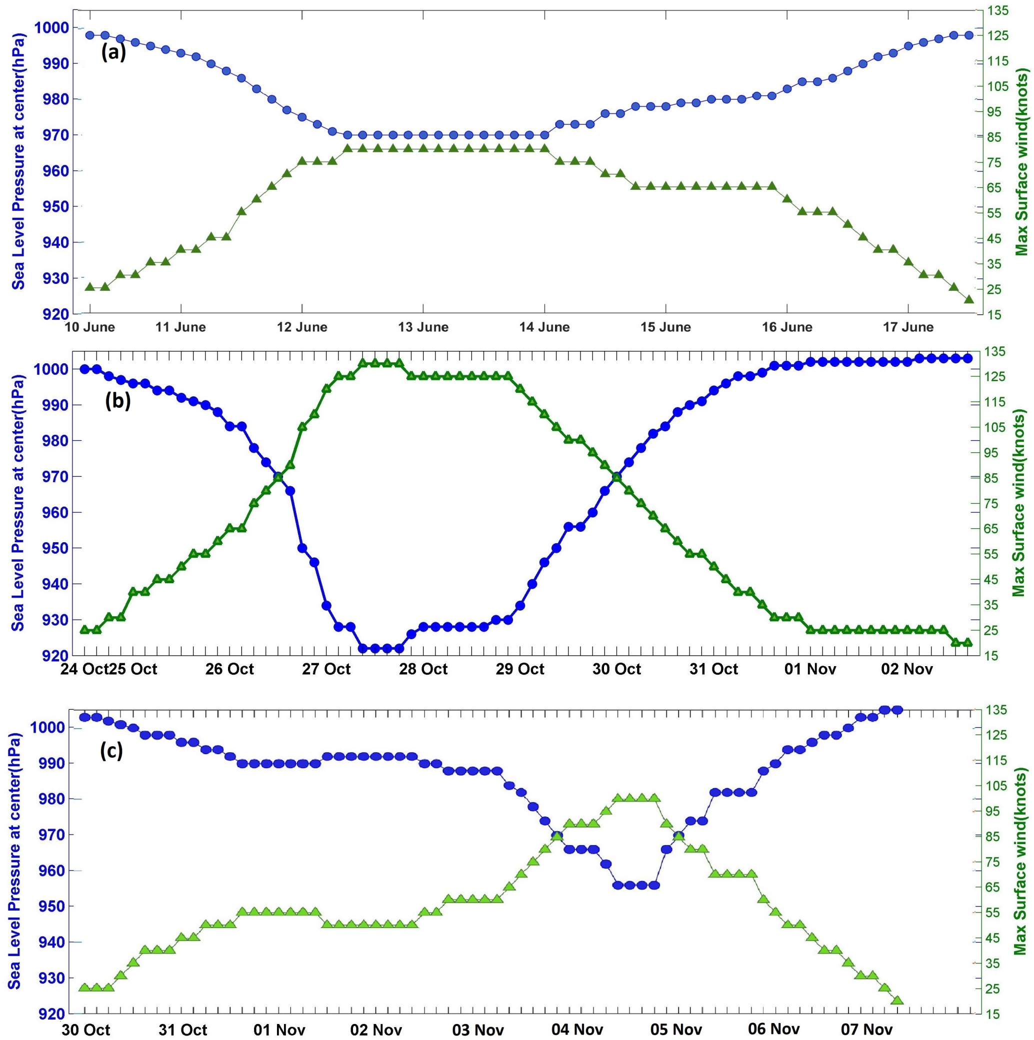

Figure 2. The sea level pressure at the center and the variations in the wind speed during the three intense recurving cyclones: a) Vayu; b) Kyarr; c) Maha.

October over the same region. It evolved into a SuCS at 0000 UTC hours on 27 October over the east-central AS. The maximum wind speed of the cyclone was 260 kmph from 0900 UTC to 1800 UTC on 27 October within geo latitude 17.4–17.8N and longitude 67–66.3N. The lowest pressure at the center of the cyclone was 922 hPa during the same period. Figure 2b shows the sea level pressure at the center and sustained wind speed variations during SuCS Kyarr.

The ESCS Maha evolved from a depression over geo latitude 6.5N and longitude 76.2E at 0600 UTC hours on 28 October 2019. It was the fourth cyclonic storm of the year in 2019 and against the climatological record of 1 per year from 1891 to 2018. It intensified following the passage of Kyarr owing to a TCHP of 100–120 KJ/cm^2. It moved northwest and evolved into a Cyclonic Storm (CS) Maha at 1200 UTC hours on 30 October at latitude 9N and longitude 74.1E. It grew into an Extremely Severe Cyclonic Storm (ESCS) At 0000 UTC hours of 4 November over geo latitude 18.1N and longitude 64.8E. The peak in maximum wind speed ESCS Maha attained was 205 kmph from 1200 UTC to 2100 UTC on 4 November within geo latitudes 18.9N to 19.5N and longitudes 64.1 to 63.6E. The lowest pressure at the center was 956 hPa from 1200 UTC to 2100 UTC on 4 November. Figure 2c shows the evolution of the sustained wind speed at the surface and the pressure drops at the center of the cyclone ESCS Maha.

4. Results

The re-curving tropical cyclones have interesting distinct patterns of wind speed variation and pressure drop at the center. The cyclone, Vayu exhibited two re-curvatures in its track. From the initial movement towards the north of the northwest, it re-curved towards the west and then toward the northeast. SuCS Kyarr moved in the direction of the

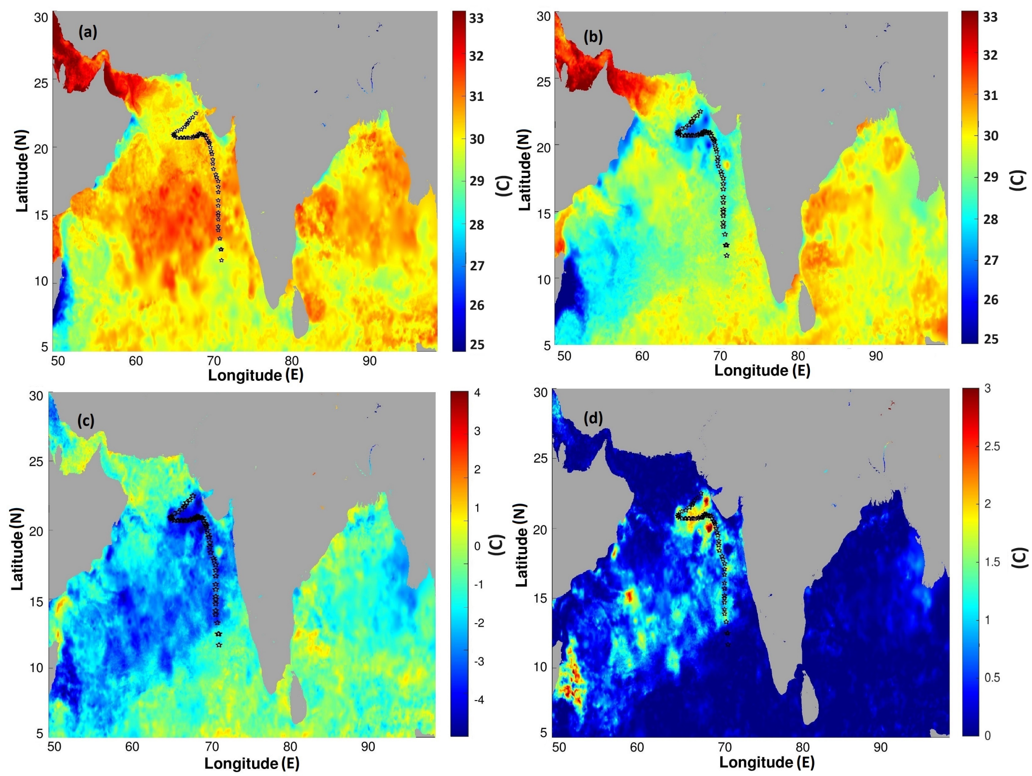

Figure 3. SST variations during VSCS VAYU. a) SST on 10 June 2019; b) SST on 16 June 2019; c) SST difference between 10 and 16 June 2019 and d) SST standard deviation between 10 June and 16 June 2019. The VSCS VAYU Track is superimposed on the SST map.

northeast initially but then re-curved towards the southeast and finally dissipated moving towards the southwest. ESCS Maha re-curved from its primary course of the north to the northwest and then to the east. The two cyclones Maha and Kyarr existed side by side for four days over the AS. Climatologically, no such event of simultaneous occurrence of two cyclonic storms over AS was recorded.

4.1 VSCS Vayu

Figure 3 shows the SST variations along the cyclone track during VSCS Vayu. Figure 3a shows the SST at the genesis stage of the VSCS Vayu. This contour plot of SST on 10 June 2019 reports that the SST was in the range of 31–32° in the area when it was in its intense stage. Following the passage of VSCS VAYU on 19 June, a decrease in SST along the track can be seen as shown in Figure 3b. The difference between SST during 10 and 16 June 2019 show a decrease of 3–4° in the cyclone impact region as visible in Figure 3c. The maximum decrease of up to 8° was seen in SST along the cyclone's best track in the area along 70E from 20N to 23N where the TC was re-curving. This is the region where the highest cooling in SST has also occurred. Interestingly, close to the re-curvature zone of VSCS Vayu, the maximum variability in SST is observed for 7 days as as shown in Figure 3d.

Figure 4a shows the SST Hovmöler plot averaged between longitude 50E–95E from 3 June to 24 June 2019. The SST Hovmöler plot details the SST contours around the cyclone's best track during the life cycle of VSCS VAYU. In the upper ocean, a decrease in SST up to 3° is seen during the post-cyclone period. At the initial days of the cyclone, SST of 29.5° is seen to be closely following the region of the cyclone's best track and is marked with a black arrow pointing to the direction of movement of the cyclone. After the cyclone reached the mature stage on 14 June and afterward, the SST of 29.5° contour seemed to narrow down and bifurcate which may have led to the formation of a re-curving best track, in the final stages of dissipation on 16–17 June, the cooling down of SST to 28° may be the cause of hindering further growth of the cyclone as can be seen in Figure 4a. Enthalpy fluxes (LFH and SFH) during June 2019 are shown in Figure 4b. These fluxes are enhanced four-fold during the cyclone and along the line of the best track compared to no cyclone period days of the month. The enthalpy reached a maximum of 280 W/m^2 during the intense stage of the cyclone. Lowered heat fluxes up to 50% of that during the intense stage after 14 June, signal a lack of potential for the further growth of the cyclone and thereby dissipation on 17 June.

Figure 5 presents the Argo floats based on in situ mea-

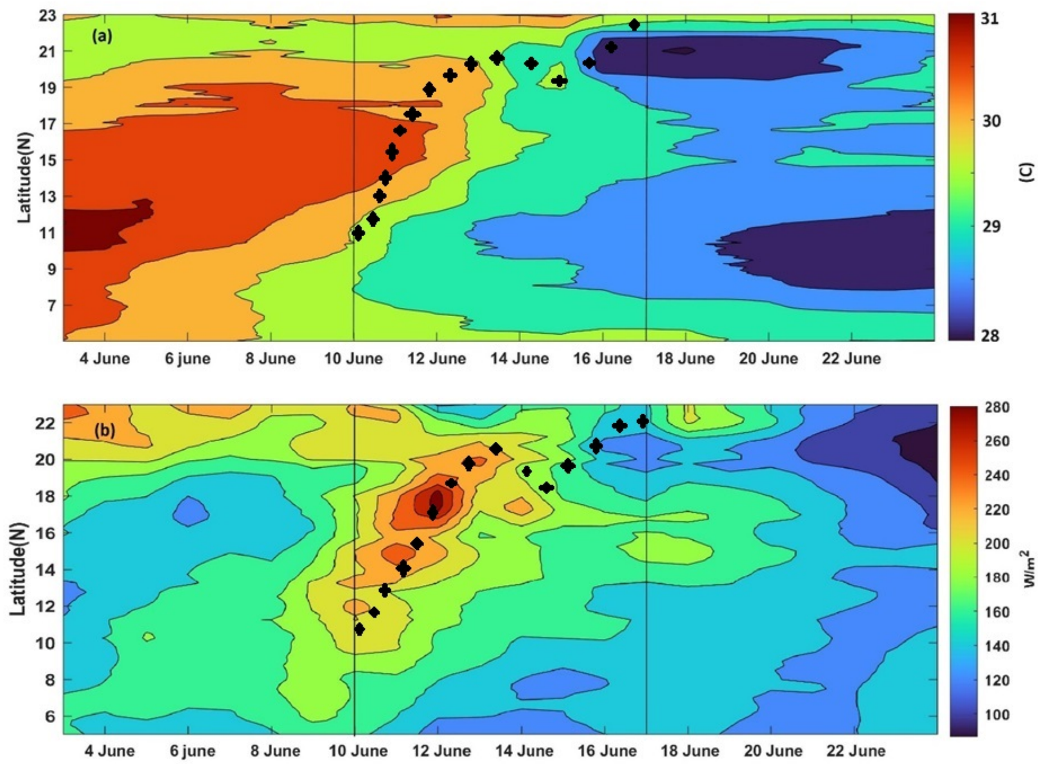

Figure 4. Hovmöler diagram of the SST (a) and averaged LHF and SHF (b) from 3 June to 24 June 2019. The black lines mark the VSCS Vayu duration from 10 June to 17 June. The cyclone's best track is superimposed on them.

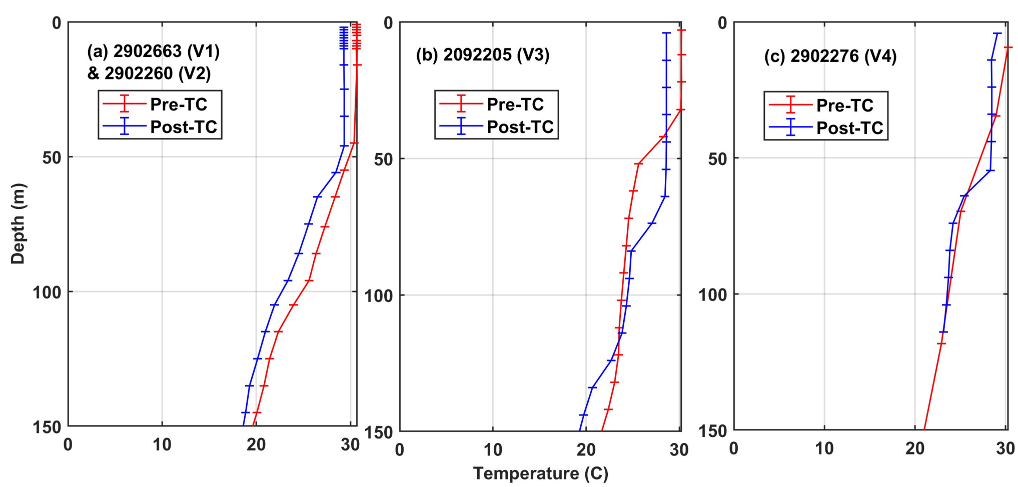

Figure 5. Subsurface temperature measurements obtained from Argo floats, left (initial stage), center, and right to the track of VSCS Vayu. The position of the Argo floats is best within 1 degree (∼ 60 nautical miles) of the position of the best track of the cyclone.

surements of the vertical temperature profile within ∼ 60 Nautical miles of the cyclone's best track. Suitable Argo floats were carefully chosen to be closest to the cyclone's best track during the cyclone's initial, mature, and final stages. Along with that, the position of the Argo floats was thoroughly scrutinized to cover the total impact region of the cyclone on the AS. Hence, the vertical temperature profile in the region left, central, and right of VSCS Vayu are studied for up to 150 m ocean depth. The horizontal bars represent one standard deviation of the temperature concerning the mean value at each depth. In the left area of the cyclone, floats 2902663, and 2902260 were used.

The central area of VSCS Vayu had float 2902205 and to the right area of the cyclone track float 2902276 located to the right of VSCS Vayu was used, which is shown in the right panel of Figure 5. Argo profiles show cooler sea surface temperature in the post-cyclone period as was also seen from satellite-based SST measurements in the initial stage of the cyclone (Argo V1). Subsequently, during the mature stage, subsurface water was warmer by 2 degrees up to ∼40 m, however, there is a mixing between the depth of 50 to 100 m. This mixing results in identical temperature profiles at the dissipating stage of the cyclone (Argo V4). This may be evidence of mixed layer deepening and re-stratification of ocean layers as indicated by Navneeth et al. (2019). This may have been caused by the upwelling of the cooler sub-surface waters to the surface and the vertical mixing of the surface and subsurface waters due to a cyclone.

4.2 SuCS Kyarr

Figure 6 presents the SST variation along the track of the SuCS Kyarr cyclone before and after its passage. Figure 6a shows SST above 27.5° in most of the region while SuCS Kyarr was developing as a tropical depression at 60E and 15N. As the cyclone moved northwestwards, SST seemed to have increased (28°–29°) in those regions. However, post-cyclone SST is decreased by 4–5° (from 29° to 25°) in Figure 6b from the region of re-curvature towards the dissipating region. This substantial difference in SST along the north of the cyclone's best track may have prevented any further northward movement but rather eastward movement up to its dissipation. There is an overall cooling of the upper ocean from the pre-cyclone period to the post-cyclone period. The maximum decrease in SST is 4° and is along the zone of re-curvature at 20N and 62E. SuCS Kyarr occurred in October 2019, which is during the post-monsoon period, so the Arabian Sea already witnessed a lowered SST due to monsoon (Khan et al., 2021). Hence, the deviation in SST is not as much as seen in the case of VSCS Vayu. However, the variability in the SST measurements was highest in the zone of re-curvature of the cyclone as in the case of VSCS Vayu.

Figure 7a–b represent the SST Hovmöler plot and enthalpy fluxes (LFH and SFH) plots averaged between longitudes 5 and 30N from 17 October 2019, 7 days before the cyclone to 9 November, 7 days after the dissipation of cyclone in 2019. The SST seems to have guided the cyclone track as it is along the 28° contours, the cyclone track moved. It re-curved around 20N, the regions where enthalpy fluxes were higher than 120 W/m^2, and followed the movement of cyclone best track. This feature is marked

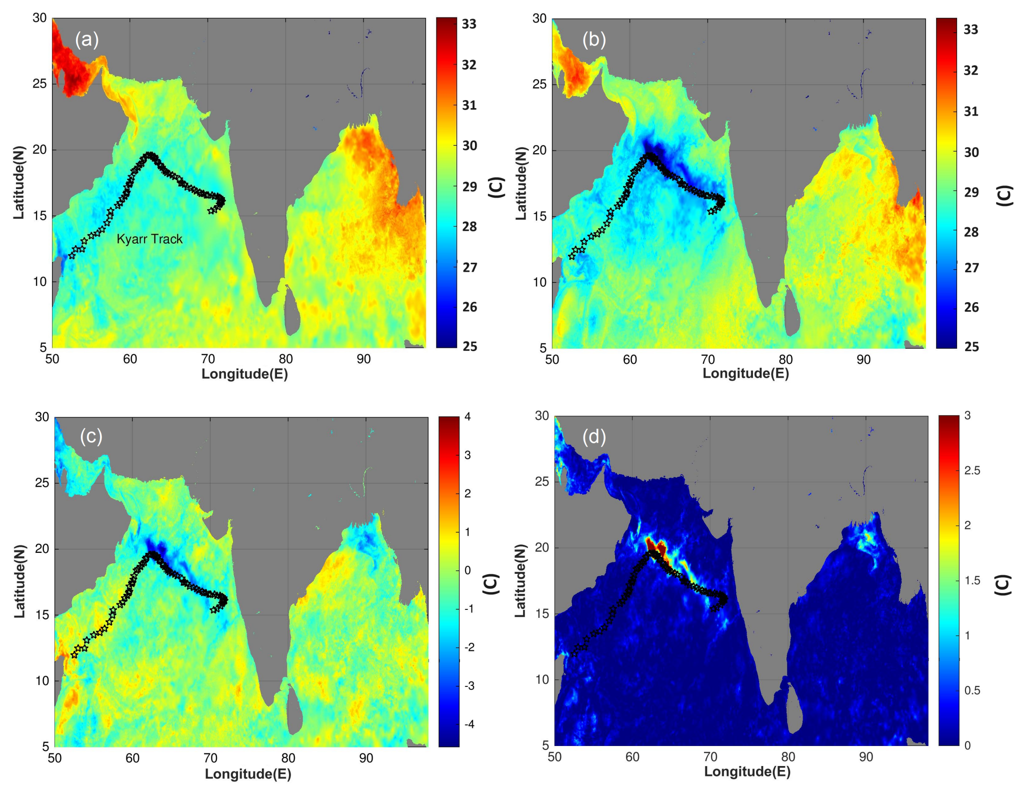

Figure 6. Variations in SST during SuCS Kyarr: a) SST on 24 October 2019; b) SST on 2 November 2019; c) Difference between SST on 24 October and 2 November 2019 and d) Standard deviation of SST between 24 October and 2 November 2019. The SuCS Kyarr Track is superimposed on the SST map.

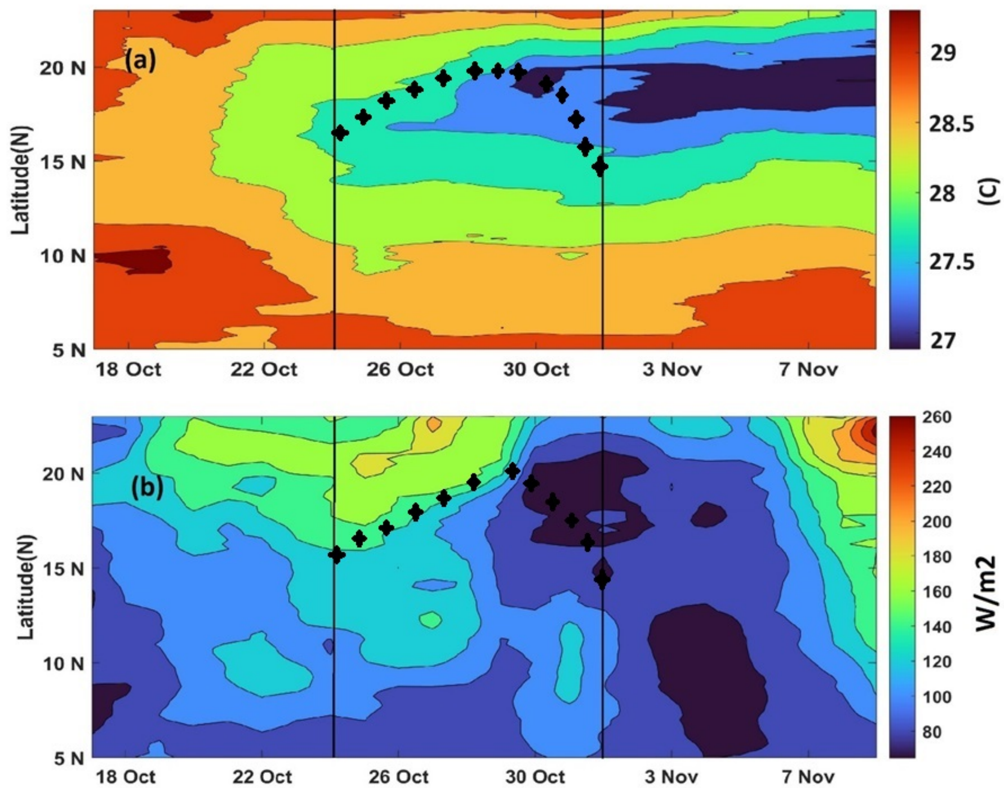

Figure 7. Hovmöler diagram of the a) SST; b) averaged LHF and SHF; from 17 Oct to 9 Nov 2019. The black lines mark the SuCS Kyarr duration from 24 Oct to 2 Nov. The Maha track is superimposed on them.

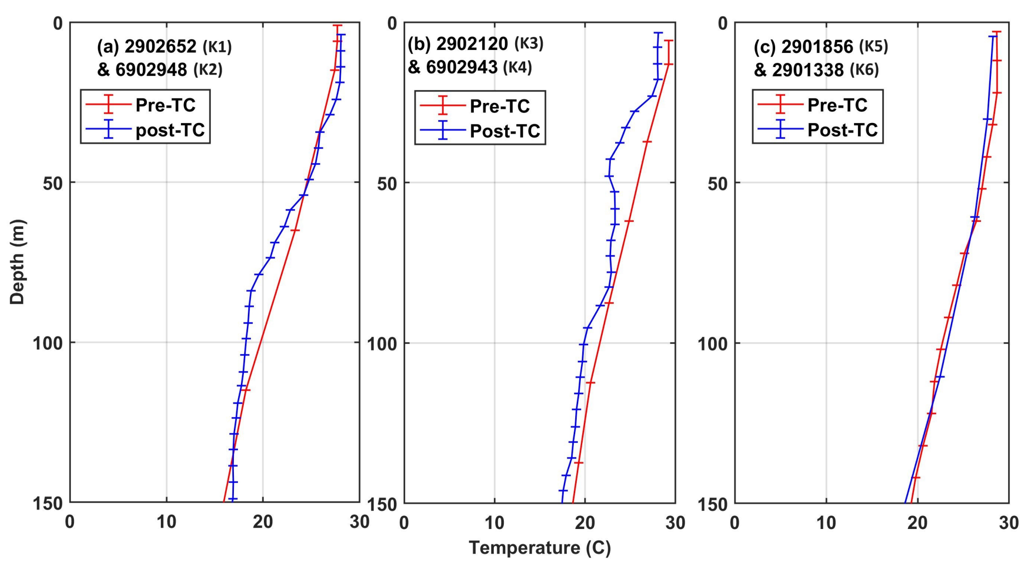

Figure 8. Subsurface temperature measurements obtained from Argo floats, left (initial stage), center (mature stage), and right (dissipation stage) along the track of SuCS Kyarr. The position of the Argo floats is best within 1 degree of the position of the best track of the cyclone.

with a black arrow in Figure 7b. Enthalpy fluxes (LFH and SFH) are found to be increased about 3–5 days before SuCS Kyarr and are seen to be enhanced in a curvy pattern as the cyclone's best track re-curved starting from latitude 10N and going towards 17–18N. When the cyclone reached 18N on 30 October, the enthalpy fluxes were lowered to 80

W/m^2 which could not fuel enough further development and the cyclone decayed. The SuCS Kyarr seemed to have been pulled from lower flux regions at 10N at about 120 W/m^2 towards 20N at about 220 W/m^2.

The in-situ measurements obtained from Argo floats showing the vertical profile of temperature during SuCS Kyarr are shown in Figure 8. Argo floats within 1-degree latitude from the cyclone's center were carefully scrutinized for this study. Temperature profiles of the subsurface waters in and around the best track of SuCS Kyarr during the cyclone life cycle are obtained. Pre-cyclone and post-cyclone temperature profiles to the left of the cyclone were obtained from floats 2902652 and 6902948 and are shown in the left panel of the figure. The central region temperature profile of SuCS Kyarr was retrieved from two floats (2902120 and 6902943) and is shown in the central panel. Two floats (2901856 and 2901338) were positioned to the right of SuCS Kyarr. Just as with VSCS Vayu, SuCS Kyarr also indicates an expansion of the mixed layer to a depth of 150 meters in the central and right regions. Cooling at the surface levels was noted in the left and central areas following the cyclone. At the sub-surface levels, cooler sea conditions seem to prevail from 50 to 100 m in the post-cyclone conditions. The subsurface heating (below 50 m) is seen to have moved upwards in the subsequent central Argo (above 50 m) and is then released into the atmosphere.

4.3 ESCS Maha

Figure 9 shows the SST measurements along the cyclone best track of ESCS MAHA. Figure 9a displays sea surface temperatures ranging from 26 to 30°C over the AS, on 30 October 2019. After the dissipation of the cyclone on 2 November 2019, SST decreased to about 2–3° along the cyclone track. The zone of the maximum reduction in SST is around the cyclone re-curvature region around 18N and 62E. SST deviation is less compared to the earlier two cyclones VSCS Vayu and SuCS Kyarr. It may be because cyclone Maha developed during the dissipating phase of the existing cyclone Kyarr. Due to this reason, SST was lowered. This is visible in Figure 9a–b, the area encompassing the region of lowered values of SST around the re-curvature zone of the cyclone best track is larger. The cooling in SST due to post-cyclone effects of SuCS Kyarr is reflected in

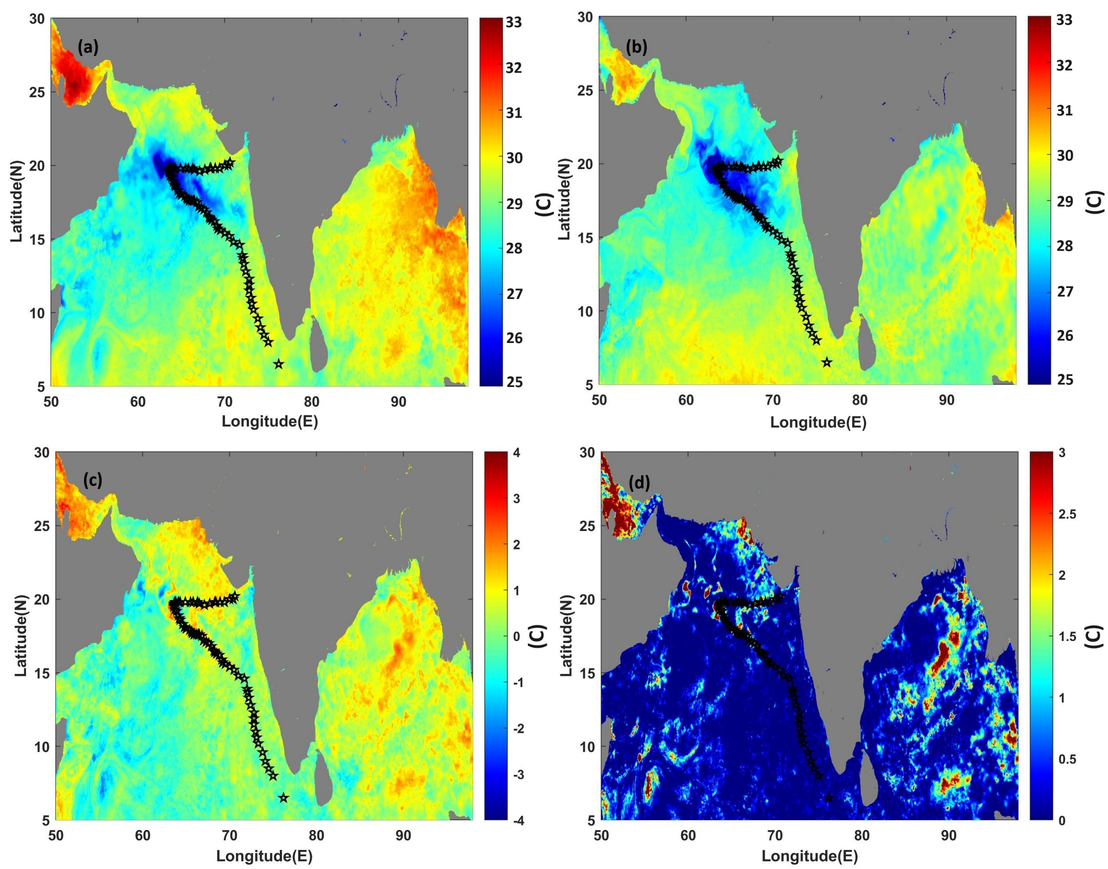

Figure 9. Variations in SST over Arabian Sea during ESCS Maha; a) SST on 30 October 2019; b) SST on 7 November 2019; c) Difference of SST between 30 October and 7 November 2019, and d) Standard deviation in SST between 30 October and 7 November 2019. The ESCS Maha Track is superimposed on the SST map.

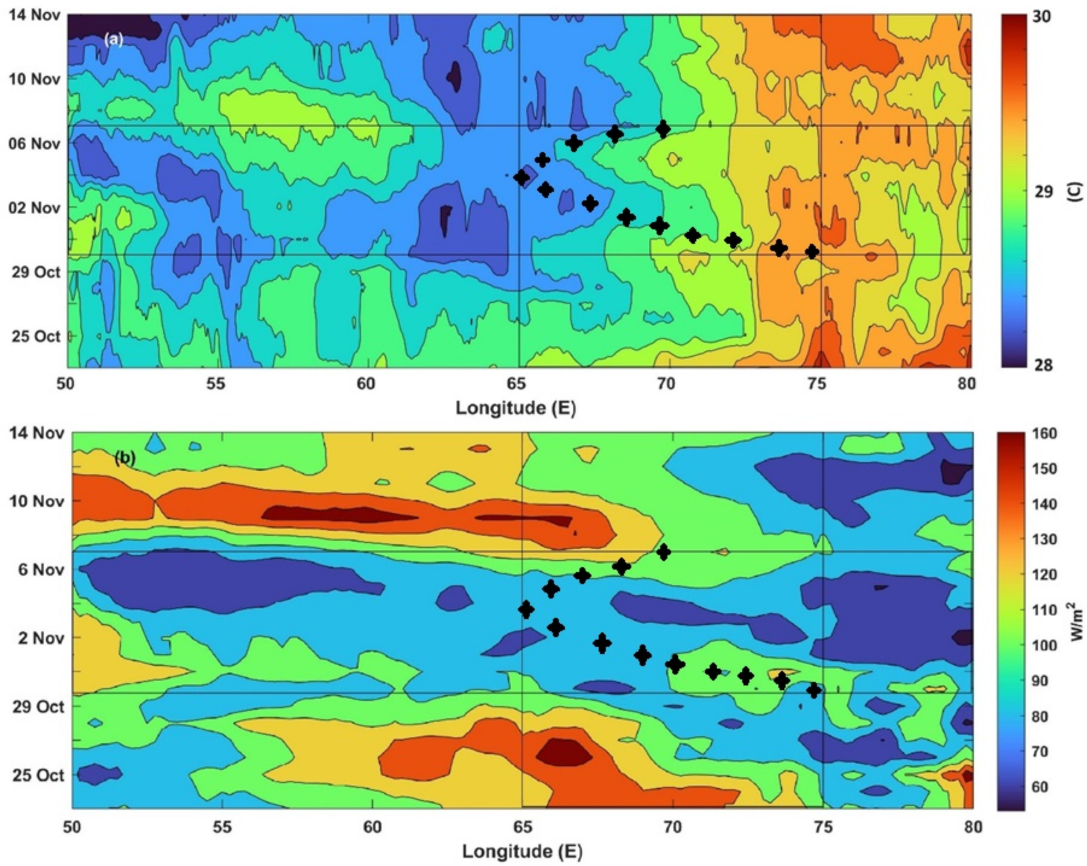

Figure 10. Hovmöler diagram of the a) SST; b) averaged LHF and SHF; from 24 October to 14 November 2019. The horizontal black lines mark the duration of ESCS Maha from 30 October to 7 November. The cyclone's best track is superimposed on them.

the overall decrease in SST for the whole Arabian Sea. Accompanying this case, the variability in pre-cyclone and post-cyclone SST is lesser as seen in Figure 9c. but, the maximum variability in SST (1–3°) has happened in the zone of re-curvature of the cyclone where there is a maximum decrease in SST.

Figure 10 showcases the Hovmöler diagram of the SST and the total enthalpy fluxes averaged between latitudes 5N and 30N from 30 October to 7 November 2019. The SST Hovmöler plot depicts the closely moving SST contour patterns during the life cycle of ESCS Maha. Closed SST contours of SST value 29° seem to follow the evolution of cyclone best track movement in Figure 10a as seen in the case of the earlier two re-curving cyclones. Figure 10a also shows SST during pre-cyclone and post-cyclone periods. Prior cyclone warmer SST forcing a wave pattern as the cyclone moves from longitude 80E in the northwest direction is visible in Figure 10a and is marked with a black arrow. Re-curving cyclone region and its near easterly movement after reaching longitude 65E is seen to have cooled down SST by $\sim 2°$. Figure 10b shows Enthalpy fluxes (LFH and SFH) before, during, and after the propagation of the cyclone over AS. These fluxes have relatively lower values compared to the other two cyclones in 2019 investigated in this study. Enthalpy fluxes have values of 80–100 W/m^2 over the cyclone impact region marked by black lines in Figure 10b. The lesser values of fluxes also are evidence of upwelling due to the earlier existing cyclone SuCS Kyarr.

Figure 11 shows the sub-surface temperature profiles obtained from Argo floats within 1 degree from the center of the track of ESCS Maha. The vertical profiles of temperature in the left, central, and right regions of the cyclone are shown in the left, central, and right panels respectively. The vertical temperature profile in the left region of ESCS Maha during the pre-and post-cyclone period was retrieved from float 2902395. The central region temperature profile of ESCS Maha was obtained from float 2902199. To the right of the ESCS Maha track, float 2902275 was used. The left, center, and right floats also were chosen during the initial, mature, and decaying stages of the cyclone respectively. The temperature profile to the left of ESCS Maha shows the deepening of the mixed layer up to 100 m depth. The pre- and post-cyclone temperature profiles remain identical. Argo float at the central region exhibits warming near

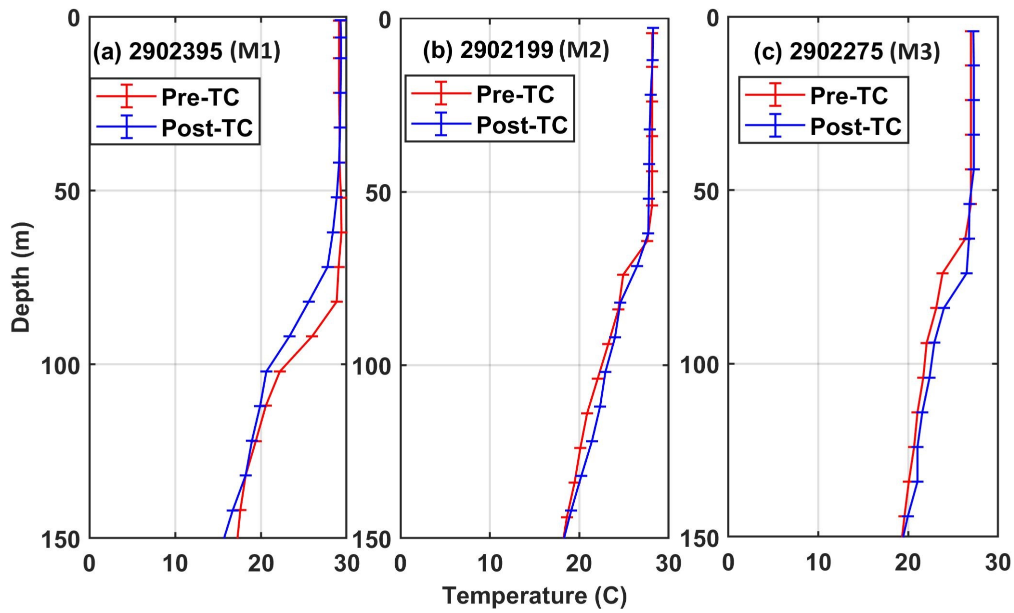

Figure 11. Subsurface temperature measurements obtained from Argo floats, left (initial stage), center (mature stage), and right (dissipation stage) to the track of ESCS Maha. The position of the Argo floats is best within 1 degree of the position of the best track of the cyclone

150 m depth in the thermocline region compared to that at the initial stage of the cyclone. The temperature profile to the right of the cyclone shows subsurface warming at all depths. This may have been caused by the upwelling of cold waters to the surface and thereby warm waters replacing the sub-surface waters.

5. Discussion

The variation of SST and enthalpy fluxes which includes both flux: latent heat and sensible heat was analyzed along the tracks of three re-curving cyclones VSCS Vayu, SuCS Kyarr, and ESCS Maha over the Arabian Sea in the year 2019. All of the TCs exhibited both slower and faster translation speeds. VSCS Vayu was the slowest with a translational speed of 10 knots (18 mph) and ESCS MAHA was the fastest-moving tropical cyclone amongst all three with a translational speed of 13 knots (24 mph). Price (1981) has categorized the hurricanes as per the translation speed of about less than 18 and more than 22 kph into slow-moving and rapidly moving TCs respectively. A recent study focused on the translational speed global slowdown of tropical cyclones, reports that due to increasing warming of the atmosphere and changes in the ambient wind, there is a priori possibility of slower translation speeds of TCs (Kossin, 2018). Kossin reports that the velocity slowdown magnitude varies substantially by location (latitude and region). Interestingly, it is observed that anthropogenic emissions-induced atmospheric circulations are the cause of these unexpected changes. The slow-moving cyclones are highly dangerous to local land regions because of the heavy rain rate.

The global warming-associated changes in tropical cyclone activity are highly influenced by the sea surface temperature change (Zhang et al., 2019). They have also found that TC frequency will increase with cooler SST pools. Our study corroborates similar findings where the cyclone best track is found to evolve along the cooler SST contours of 29–29.5° (Figures 4a, 7a, and 10a) instead of maximum SST regions. The SST along the re-curvature region of cyclones was seen to reduce by 3–9° as can be observed from the SST data plots for the three TCs (Figures 3b,6b and 9b). The maximum change in the SST is found to occur during slower cyclone VSCS Vayu (9°). In contrast to SST dealing with the post-cyclone and pre-cyclone conditions, all three cyclones exhibited cooler SST in the post-cyclone conditions and warmer SST during pre-cyclone conditions. The proportion change in the SST up to 8° matches well with past works (Guan et al., 2014; Zhang et al., 2019; Chandra and Kumar, 2021) but is slightly higher by 1 to 2° in our findings.

Tropical cyclones can cause upwelling of the cold subsurface water and displace the existing warm surface water thereby driving a strong vertical mixing in the upper ocean (Korty et al., 2008). This is evident in the Hovmöler plot of enthalpy fluxes Figure 10b that, despite the evolution of ESCS Maha during the dissipation stage of SuCS Kyarr, the fluxes show a cooling period. Mixing is also evident in the re-curvature zones where a decrease in the SST has occurred. The decrease in the SST was too manifest in the Argo profiles after the TC passage. During the post-cyclone period, the ocean using geostrophic adjustment processes adjusts itself toward equilibrium thus, generating durable internal axial currents. These currents rotate at the near-inertial frequencies which drive the near-inertial pumping process and vertically directed pruning, thus acting as the driver of intense vertical mixing of the Upper Ocean during a post-cyclone condition (Jaimes et al., 2015; Kossin, 2018; Zhang et al., 2019; Chandra and Kumar, 2021). The Argo profile provided details about the decrease in temperature based on the mixed layer depth and the increase in temperature at a depth of 100 m and more which reveals warming. This phenomenon can also be explained based on the upwelling of colder water to the surface and the vertical mixing of ocean layers which is further incited by wind stress associated with a cyclone.

In situ observations obtained from Argo floats, moored buoys, etc., reveal the distinct nature of the near-surface (up to 50 m depth), thermocline (50–100 m) and subsurface (100 to 150 m) features of the temperature and salinity play in modifying upper ocean dynamics during a tropical cyclone (Knaff et al. 2013; Kossin, 2018; Navneeth et al., 2019). The present results show that the near-surface temperature for VSCS Vayu and SuCS Kyarr has decreased and the sub-surface temperature has increased. In the case of ESCS Maha, the vertical temperature profile remains identical. In the case of Vayu, the cooling extended up to a depth of 100 m along the best track, higher than both to the left and the right of the track. Stronger cooling observed during the cyclones is more pronounced in the left and center Argo profiles for VSCS Vayu and SuCS Kyarr (Figure 5 and Figure 8). A study of upper ocean characteristics during cyclone Nisarga over the Bay of Bengal using in situ observations reported that for the intense TCs (Categories 4 and 5), the sub-surface warming and the near-surface cooling were mostly associated with the vertical mixing. The dominating factors for this change during the cyclone were enthalpy fluxes associated with upwelling which corroborates the findings of earlier researchers (Maneesha et al., 2012). They have reported measurements of inertial currents to the right of a Category 4 cyclone that resulted in vertical mixing due to turbulent fluxes (LHF and SHF) and deepening of mixed layer which is evident in our study of VSCS Vayu and SuCS Kyarr.

Enhanced heat fluxes at the ocean surface enable the cooling in SST during a cyclone and the upwelling of cold deep ocean water. Enhanced heat fluxes along the track of VSCS Vayu were observed during all stages of intensification (Figures 4b). Regions of higher enthalpy fluxes were the dominant pull factor for the evolution of cyclone best track during SuCS Kyarr Figure 7b. Previous studies on TC intensification observed a higher value of air-sea enthalpy heat fluxes that contributed significantly to the faster strengthening of the TCs Nisarg, Phailin, and Hudhud, in the Bay of Bengal, which is consistent with the present finding on the TC faster strengthening over the area of increase heat fluxes (Maneesha et al., 2012; Navneeth et al., 2019). Jaimes et al. (2015) examined the upper ocean characteristics for TC Earl (Category 4) using enthalpy fluxes and found that the fluxes increased 6 times during the intense stage of the cyclone. Our results validate their findings. Because of the changing dynamics of the Arabian Sea cyclones and the suddenly exhibited re-curving feature, the role of SST, vertical temperature profiles, and enthalpy fluxes would play a key role in deepening their understanding.

6. Conclusion

Arabian Sea witnessed a never-seen occurrence of four severe cyclones in 2019 against the climatological record of one per year 1891–2018 (IMD, 2020). These severe cyclones exhibited re-curvatures of cyclone best track, which made them potentially difficult to predict and hence more dangerous. In this view, studying the upper ocean characteristics, and understanding the dynamics of the subsurface ocean from in situ measurements becomes important. With this aim, three intense cyclones VSCS Vayu, SuCS Kyarr, and ESCS Maha were studied. Previously there was no such event of simultaneous occurrence of two cyclones over the Arabian Sea during the period 1961–2018.

Sea Surface Temperature (SST) reductions to up to 2–8° in the region of re-curvature are seen. Maximum reduction in SST has occurred during slow-moving cyclone VSCS Vayu with a translational speed of 10 knots. Enthalpy fluxes increased 4 fold along the cyclone best track from 80 J/kg to 280 J/kg on average during Vayu and Kyarr. In the case of the existence of two cyclones (SuCS Kyarr and ESCS Maha) over AS, colder regions with fewer enthalpy fluxes are seen in the case of Maha which developed later. Subsurface ocean water reports a cooling in the surface levels up to 50 m. There is deepening of the mixed layer near the thermocline may be caused due to turbulent mixing. The sub-surface water from 100 m to 150 m depth shows warming that is caused by colder water being displaced to the surface during the post-cyclone time. This work is an effort to fill the gap of fewer studies of cyclones over the Arabian Sea. Our study may help us understand the role of dynamics of the Arabian Sea that play an important role in increasing the number and intense tropical cyclones in a future scenario.

Acknowledgments

The authors are thankful to the Director, of the Indian Institute of Tropical Meteorology, Pune for encouragement and for providing basic infrastructure to carry out the present work. The authors are also thankful to the Director, of the Indian Institute of Geomagnetism, Navi Mumbai for lending support to this study. The authors are also thankful to the DGM, India Meteorological Department for his support and encouragement. The author, AD is thankful to the Science and Engineering Research Board (SERB), Department of Science and Technology (DST) for their support with funds (File no. PDF/2020/002004).

Declaration of competing interest

Adarsh Dube reports that financial support was provided by the Science and Engineering Research Board. Adarsh Dube reports a relationship with the Indian Institute of Tropical Meteorology that includes non-financial support. Adarsh Dube reports a relationship with the India Meteorological Department that includes non-financial support. T Dharmaraj reports a relationship with the Indian Institute of Tropical Meteorology that includes non-financial support. Rajesh Singh reports a relationship with the Indian Institute of Geomagnetism that includes non-financial support. Ajeet Kumar Maurya reports a relationship with the University of Lucknow that includes non-financial support.

References

Aiyyer, A., 2015. *Recurving western North Pacific tropical cyclones and midlatitude predictability*, Geophys. Res. Lett. 42, 7799–7807. https://doi.org/10.1002/2015GL065082

Shyamala, B., Sudevan, S., Shinde, G.M., Burte, M.D., 2001. *Behaviour of recurving cyclonic storms in the Arabian Sea as a response to atmospheric interactions*, MAUSAM 52(3), 469–478. https://doi.org/10.54302/mausam.v52i3.1718

Bhaskar Rao, D.V., Hari Prasad, D., Srinivas, D., 2009. *Impact of Horizontal resolution and the advantages of nested domains approach in the prediction of tropical cyclone intensification and movement*, JGR 114, D11106. https://doi.org/10.1029/2008JD011623

Bongirwar, V., Rakesh, V., Kishtawal, C.M., Joshi, P.C., 2011. *Impact of satellite observed microwave SST on the simulation of tropical cyclones*. Natural Hazards 58, 929–944. https://doi.org/10.1007/s11069-010-9699-y

Cai, Y., 2022. *Enhanced Predictability of rapidly intensifying tropical cyclones over the western North Pacific associated with snow depth changes over the Tibetan Plateau*, J. Clim., 1–17. https://doi.org/10.1175/JCLI-D-21-0758.1

Cao, J., Haikun Z., Bin W., Liguang W., 2021. *Hemisphere-asymmetric tropical cyclones response to anthropogenic aerosol forcing*. Nat.Commun. 12, 6787, 1–8. https://doi.org/10.1038/s41467-021-27030-z

Chand, S. S., Walsh, K. J., Camargo, S. J., Kossin, J. P., Tory, K. J., Wehner, M. F., et al., 2022. *Declining tropical cyclone frequency under global warming*. Nature Climate Change 12(7), 655–661. https://doi.org/10.1038/s41558-022-01388-4

Cione, J.J., Uhlhorn, E.W., 2003. *Sea surface temperature variability in hurricanes: Implications concerning intensity change*. Mon. Weather Rev. 131, 1783–1796.

Craig, G. C., Gray, S. L., 1996. *CISK or WISHE as the mechanism for tropical cyclone intensification*. J. Atmos. Sci. 53, 3528–3540. https://doi.org/10.1175/1520-0469(1996)053,3528COWATM.2.0.CO;2

Crespo, J.A., Posselt, D.J., Asharaf, S., 2019. *CYGNSS Surface Heat Flux Product Development*. Remote Sens. 11, 2294. https://doi.org/10.3390/rs11192294

Dare, R.A., McBride, J.L., 2011a. *The threshold sea surface temperature condition for tropical cyclogenesis*. J. Climate 24, 4570–4576. https://doi.org/10.1175/JCLI-D-10-05006.1

Dare, R.A., McBride, J.L., 2011b. *Sea surface temperature response to tropical cyclones*, Mon. Wea. Rev., 139, 3798–3808. https://doi.org/10.1175/MWR-D-10-05019.1

Emanuel, K.A., 1986. *An air-sea interaction theory for tropical cyclones. Part I: Steady state maintenance*. J. Atmos. Sci. 43, 585–604. https://doi.org/10.1175/1520-0469(1986)043,0585:AASITF.2.0.CO;2

Evan, A.T., Camargo, S. J., 2011 *A climatology of Arabian Sea Cyclonic storms*, J. Clim. 24(1), 140–158. https://doi.org/10.1175/2010JCLI3611.1

Gautam, R., Cervone, G., Singh, R.P., Kafatos, M., 2005. *Characteristics of meteorological parameters associated with Hurricane Isabel*. Geophys. Res. Lett., 32, L04801. https://doi.org/10.1029/2004GL021559

Guan, S., Zhao, W., Huthnance, J., Tian, J., Wang, J., 2014. *Observed upper ocean response to Typhoon Megi (2010) in the northern South China Sea*. J. Geophys. Res. Oceans, 119, 3134–3157. https://doi.org/10.1002/2013JC009661

Hari, V., Pathak, A., Koppa, A., 2021. *Dual response of Arabian Sea cyclones and strength of Indian monsoon to Southern Atlantic Ocean*, Climate Dynam. 56, 2149–2161. https://doi.org/10.1007/s00382-020-05577-9

IMD (India Meteorological Department), 2020. *Report on cyclonic disturbances over North Indian Ocean during 2019*. MOES/IMD/RSMC Tropical Cyclone Rep. No. 01 (2020)/10.

IPCC, 2014. *Intergovernmental Panel for Climate Change 2014*. Synthesis Rep. Summary for Policy Makers.

Jaimes, B., Shay, L.K., Uhlhorn, E.W., 2015. Enthalpy and momentum fluxes during Hurricane Earl relative to underlying ocean features. Mon. Wea. Rev. 143, 111–131.

James P. Kossin, 2018. *A global slowdown of tropical cyclone translational speed*. Nature 104(558). https://doi.org/10.1038/s41586-018-0158-3

Katsube, K., Inatsu, M., 2016. *Response of tropical cyclone tracks to sea surface temperature in the western North Pacific*. J. Climate 29, 1955–1975. https://doi.org/10.1175/JCLI-D-15-0198.1

Khan S, Shengchun Piao, Imran U. Khan, Bingchen Xu, Shazia Khan, Muhammad Asim Ismail and Yang Song, 2021. *Variability of SST and ILD in the Arabian Sea and Sea of Oman in Association with the Monsoon Cycle*. Recent Trends in Advanced Robotic Systems. https://doi.org/10.1155/2021/9958257

Knaff, J. A., DeMaria, M., Sampson, C.R., Peak, J.E., Cummings, J., Schubert, W.H., 2013. *Upper oceanic energy response to tropical cyclone passage*. J. Climate 26, 2631–2650. https://doi.org/10.1175/JCLI-D-12-00038.1

Korty, R. L., Emanuel, K.A., Scott, J.R., 2008. *Tropical cyclone-induced upper-ocean mixing and climate: Application to equable climates*. J. Climate 21, 638–654. https://doi.org/10.1175/2007JCLI1659.1

Kotal, S.D., Bhowmik, R., Kumdu, P.K., Ananda D.K., 2008. *A statistical cyclone intensity prediction (SCIP) model for the bay of Bengal*. J. Earth Syst. Sci. 117(2), 157–168. https://doi.org/10.1007/s12040-008-0006-1

Krishnamurti, T N., Pattnaik, S., Stefanova, L., Kumar, T.S.V.V., Mackey, B.P., O'Shay, A.J., Pasch, R.J., 2005. *The Hurricane Intensity Issue*. Mon. Wea. Rev. 133, 1886–1912. https://doi.org/10.1175/MWR2954.1

Lin, I.-I., Chen, C.-H., Pun, I.-F., Liu, W.T., Wu, C.-C., 2009. *Warm ocean anomaly, air sea fluxes, and the rapid intensification of Tropical Cyclone Nargis (2008)*. Geophys. Res. Lett. 36, L03817. https://doi.org/10.1029/2008GL035815

Wahiduzzaman, M., Cheung, K.K., Jing-Jia, L., Bhaskaran, P.K., 2022. *A spatial model for predicting North Indian Ocean tropical cyclone intensity: Role of sea surface temperature and tropical cyclone heat potential*. Weather and Climate Extremes 36, 100431. https://doi.org/10.1016/j.wace.2022.100431

Ma, Z., 2018. *Examining the contribution of surface sensible heat flux induced sensible heating to tropical cyclone intensification from the balance dynamics theory*. Dynm. Atmos. Oceans 84, 33–45. https://doi.org/10.1016/j.dynatmoce.2018.09.001

Ma, Z., Fei, J., Huang, X., Cheng, X., 2015. *Contributions of surface sensible heat fluxes to a tropical cyclone. Part I: Evolution of tropical cyclone intensity and structure*. J. Atmos. Sci. 72, 120–140. https://doi.org/10.1175/JAS-D-14-0199.1

Maneesha, K., Murty, V.S.N., Ravichandran, M., Lee, T., Weidong, Y., McPhaden, M.J., 2012 *Upper ocean variability in the Bay of Bengal during the tropical cyclones Nargis and Laila*. Prog. Oceanogr. 106, 49–61. https://doi.org/10.1016/j.pocean.2012.06.006

Mohanty, S, Raghu, N., Krishna, K., O.„ Sujata P., Mohanty, U.C., Sourav S., 2019. *Role of Sea Surface Temperature in Modulating Life Cycle of Tropical Cyclones over Bay of Bengal*. Tropical Cycl. Res. Rev. 8(2), 68–83. https://doi.org/10.1016/j.tcrr.2019.07.007

Murakami, H., Vecchi, G.A., Underwood, S., 2017. *Increasing frequency of extremely severe cyclonic storms over the Arabian Sea*. Nature Clim. Chang. 7, 885–889. https://doi.org/10.1038/s41558-017-0008-6

Navaneeth, K.N., Martin, M.V, Joseph, K.J., Venkatesan, R., 2019. *Contrasting the upper ocean response to two intense cyclones in the Bay of Bengal*. Deep Sea Res. Pt. I 147, 65–78. https://doi.org/10.1016/j.dsr.2019.03.010

Neetu, S., Lengaigne, M., Vincent, E.M., Vialard, J., Madec, G., Samson, G., Ramesh Kumar, M.R., Durand, F., 2012. *Influence of upper-ocean stratification on tropical cyclone-induced surface cooling in the Bay of Bengal*J. Geophys. Res. Ocean. 117, C12020. https://doi.org/10.1029/2012JC008433

Park, J.J., Y.-O. Kwon, Price, J.F., 2011. *Argo array observation of ocean heat content changes induced by tropical cyclones in the north Pacific*. J. Geophys. Res. 116, C12025. https://doi.org/10.1029/2011JC007165

Price, J.F., 1981. *Upper ocean response to a hurricane*. J. Phys. Oceanogr. 11, 153–175. https://doi.org/10.1175/1520-0485(1981)011<0153:UORTAH>2.0.CO;2

Sun, Y., Zhong, Z., Tim, L., Lan, Y., Yijia, H., Hongchao, W., Haishan, Ch., Qianfeng, L., Chen, M., Qihua, L., 2017. *Impact of ocean warming on tropical cyclone size and its destructiveness*. Sci. Rep. 7, 8154. https://doi.org/10.1038/s41598-017-08533-6

Zhang, B., Renhe, Z., Pinker, R.T., Yerong, F., Changchun, N., Guan, Y., 2019. *Changes of tropical cyclone activity in a warming world are sensitive to sea surface temperature environment*. Environ. Res. Lett. 14, 124052. https://doi.org/1748-9326/ab5ada

Zhao, H., Duan, X., Raga, G.B., Klotzbach, P.J., 2018. *Changes in characteristics of rapidly intensifying western North Pacific tropical cyclones related to climate regime shifts*. J. Clim. 31, 8163–8179. https://doi.org/10.1175/JCLI-D-18-0029.1